



OPEN

## Extrachromosomal DNA formation enables tumor immune escape potentially through regulating antigen presentation gene expression

Tao Wu<sup>1,2,3,6</sup>, Chenxu Wu<sup>1,2,3,6</sup>, Xiangyu Zhao<sup>1</sup>, Guangshuai Wang<sup>1</sup>, Wei Ning<sup>1</sup>, Ziyu Tao<sup>1</sup>, Fuxiang Chen<sup>4</sup> & Xue-Song Liu<sup>1,5</sup>✉

Extrachromosomal DNA (ecDNA) is a type of circular and tumor specific genetic element. EcDNA has been reported to display open chromatin structure, facilitate oncogene amplification and genetic material unequal segregation, and is associated with poor cancer patients' prognosis. The ability of immune evasion is a typical feature for cancer progression, however the tumor intrinsic factors that determine immune evasion remain poorly understood. Here we show that the presence of ecDNA is associated with markers of tumor immune evasion, and obtaining ecDNA could be one of the mechanisms employed by tumor cells to escape immune surveillance. Tumors with ecDNA usually have comparable TMB and neoantigen load, however they have lower immune cell infiltration and lower cytotoxic T cell activity. The microenvironment of tumors with ecDNA shows increased immune-depleted, decreased immune-enriched fibrotic types. Both MHC class I and class II antigen presentation genes' expression are decreased in tumors with ecDNA, and this could be the underlying mechanism for ecDNA associated immune evasion. This study provides evidence that ecDNA formation is an immune escape mechanism for cancer cells.

The immune system plays a crucial role in the protection and fight against cancer cells<sup>1,2</sup>. Immunoediting, which includes three temporally distinct stages, termed elimination, equilibrium, and escape, has been proposed to explain the interactions between cancer cells and the immune system during the evolution of cancer<sup>3-5</sup>. The mechanisms responsible for the escape of tumor cells from immunosurveillance are not fully understood. Potential tumor intrinsic immune evasion mechanisms include: impaired antigen presentation machinery (such as B2M mutation, decreased antigen presentation gene expression<sup>6-8</sup>), overexpressed immune checkpoints or their ligands such as programmed death-ligand 1 (PD-L1) on cancer cells<sup>9</sup>. In addition, secreting of immune inhibitory cytokines, such as TGF- $\beta$ , remarkably reshape the tumor immune microenvironment<sup>10,11</sup>.

Extrachromosomal DNA (ecDNA) is a type of tumor specific DNA element that is circular and about 1–3 Mb in size. Since the 1960s, double minute chromosomes have been observed in the metaphase spreads of human cancer cells<sup>12</sup>. Later these DNA elements without centrioles and telomeres are found to be circular, a few Mb in size, and their size but not their number is stable during the proliferation of cancer cells<sup>13</sup>. With the recent advance of sequencing and bioinformatics techniques, ecDNA has been found to be prevalent in various types of cancers, however ecDNA is rarely detected in normal tissues, suggesting the presence of ecDNA is a specific feature for some cancer cells<sup>14</sup>. EcDNA promotes accessible chromatin (open chromatin) formation, facilitates oncogene amplification, drives genetic heterogeneity, and is associated with poor prognosis in multiple types of cancer<sup>15-17</sup>.

<sup>1</sup>School of Life Science and Technology, ShanghaiTech University, Shanghai 201203, People's Republic of China. <sup>2</sup>Shanghai Institute of Biochemistry and Cell Biology, Chinese Academy of Sciences, Shanghai, People's Republic of China. <sup>3</sup>University of Chinese Academy of Sciences, Beijing, China. <sup>4</sup>Department of Clinical Immunology, Ninth People's Hospital, Shanghai Jiao Tong University School of Medicine, Shanghai 200011, People's Republic of China. <sup>5</sup>School of Life Science and Technology, ShanghaiTech University, 230 Haik Road, Shanghai 201210, People's Republic of China. <sup>6</sup>These authors contributed equally: Tao Wu and Chenxu Wu. ✉email: liuxs@shanghaitech.edu.cn

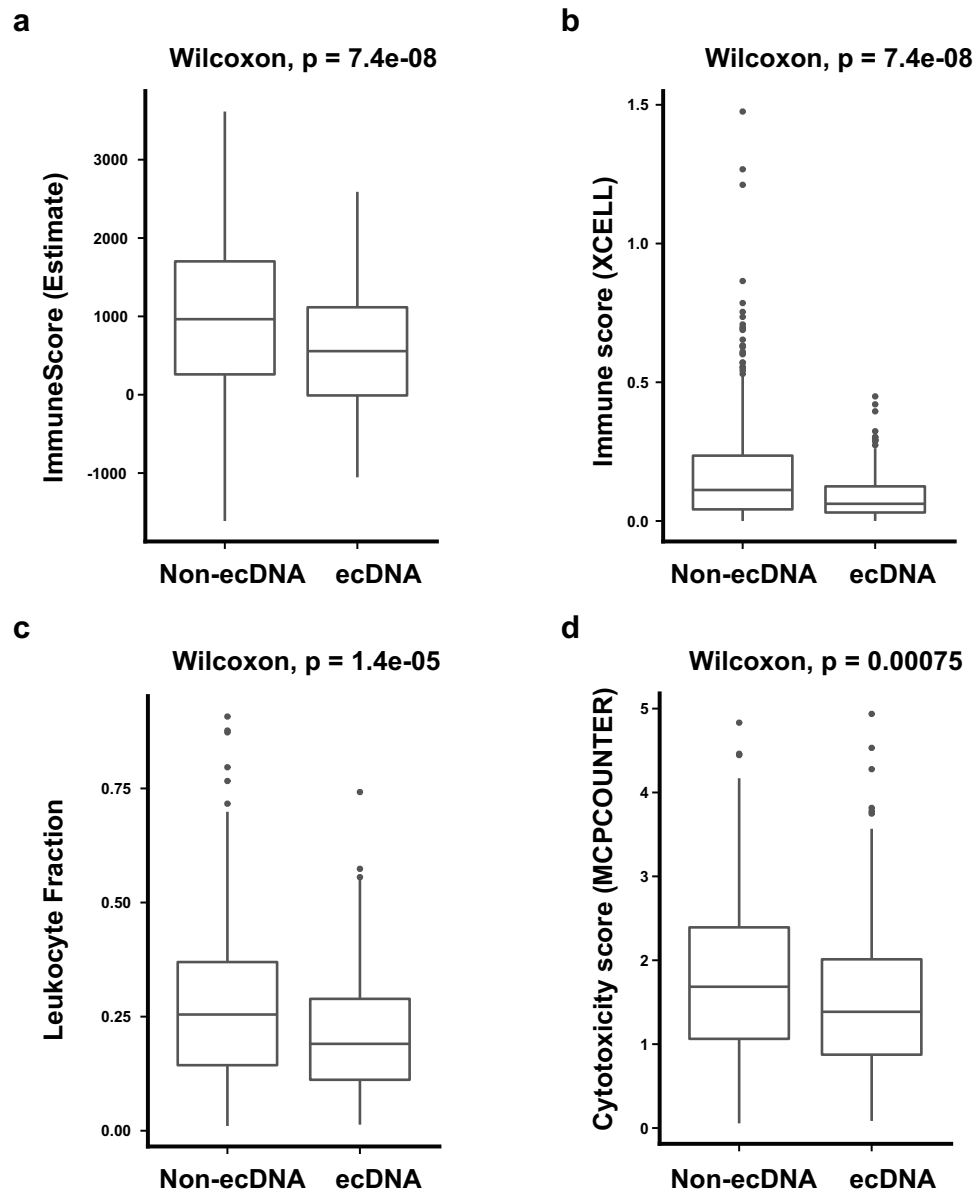


**Figure 1.** ecDNA and tumor immune infiltration scores. (a–d) Comparisons of immune infiltration scores quantified by different methods between tumors with and without ecDNA. (a) Estimate ImmuneScore; (b) XCELL Immune score; (c) Leukocyte fraction, (d) MCPCounter cytotoxicity score. Wilcoxon test *P* values are shown.

Somatic DNA alterations are major determinants of cancer phenotypes, including immune phenotypes. EcDNA formation is a type of somatic DNA alteration. We hypothesize that ecDNA formation could be one mechanism for cancer cells to evade immune surveillance.

## Results

**EcDNA and tumor immune cell infiltration status.** For this study, we select cancer patient samples with both WGS and gene expression data for analysis. The status of ecDNA in specific samples was determined based on WGS data as previously described<sup>17</sup>. In total, 1684 samples with ecDNA status and gene expression information are available for analysis (Supplementary Fig. S1).

First we investigate the correlation between the presence of ecDNA and tumor immune infiltration status. The immune infiltration status was determined using gene mRNA expression data. Multiple methods have been applied in the quantification of tumor immune status, including TIMER, CIBERSORT, Xcell, MCPcounter, Quantiseq and Estimate<sup>18–23</sup>. With different methods, tumors with ecDNA consistently show significantly decreased immune scores (Fig. 1a–c and Supplementary Fig. S2). Importantly, the cytotoxic T cell (CD8<sup>+</sup>) levels and cytotoxic scores are significantly decreased in tumors with ecDNA (Fig. 1d and Supplementary Fig. S3). The composition of different immune cells was calculated using gene expression data with multiple different methods,

including marker gene-based methods (Xcell and MCPcounter) or deconvolution-based methods (Cibersort, Timer, and Quantiseq). Multiple types of immune cells including B cell, NK cell and T cell show significantly decreased composition in tumors with ecDNA in TCGA pan-cancer dataset as a whole (Fig. 2a), or in separate cancer types, such as STAD (Stomach adenocarcinoma), SKCM (Skin cutaneous melanoma), HNSC (Head and neck squamous cell carcinoma) (Fig. 2b and Supplementary Fig. S3).

**EcDNA and tumor immune typing.** Tumor immune typing was performed according to two known studies<sup>24,25</sup>. Thorsson et al. used consensus clustering based on scored immune expression signatures to cluster cancer samples into six immune subtypes—wound healing, IFN- $\gamma$  dominant, inflammatory, lymphocyte depleted, immunologically quiet, and TGF- $\beta$  dominant<sup>25</sup>. In tumors with ecDNA, lymphocyte depleted type is up-regulated, while inflammatory and TGF- $\beta$  dominant types are down-regulated (Fig. 3a). Bagaev et al. used unsupervised dense Louvain clustering based on ssGSEA (single-sample gene set enrichment analysis) scores of 29 Fges (functional gene expression signatures) of immune and stromal related genes to cluster cancer samples into four distinct microenvironments: (1) immune-enriched, fibrotic (IE/F); (2) immune-enriched, non-fibrotic (IE); (3) fibrotic (F); and (4) immune-depleted (D)<sup>24</sup>. In tumors with ecDNA, fibrotic immune-enriched type of TME (IE/F) is dramatically decreased, while immune desert type TME (D) is significantly up-regulated (Fig. 3b). These tumor immune typing results further validate the observation that the presence of ecDNA is associated with decreased immune cell infiltration status.

**EcDNA and tumor immune escape.** Expression of immune inhibitory immune checkpoint genes, such as PD-L1, CTLA4 is significantly down-regulated in tumors with ecDNA (Fig. 4a and Supplementary Fig. S4), suggesting the immune evasion of tumors with ecDNA is not through stimulating immune checkpoint signaling. This also implicates that immune checkpoint inhibitor therapy alone may not work in tumors with ecDNA.

**Antigen presentation and ecDNA mediated immune escape.** Tumors with ecDNA show decreased immune cell infiltration, suggesting a decrease of immunogenicity in ecDNA-containing tumor cells. The immunogenicity of tumor cells determines the tumor associated immune response, and the antigenicity encoded by neoantigenic mutations is an important determinant of tumor immunogenicity<sup>26</sup>. Tumors with ecDNA show comparable TMB and neoantigen counts, suggesting a comparable antigenicity (Fig. 4b and Supplementary Fig. S5). This implies that the decreased immunogenicity of ecDNA-containing tumors was not caused by impaired antigenicity.

Antigen presentation efficiency is another important determinant of tumor immunogenicity<sup>26</sup>. The function of MHC class I antigen presentation pathway is to display peptide fragments of proteins from within the cell to cytotoxic T cells; MHC Class II molecules are normally found only on professional antigen-presenting cells such as dendritic cells, mononuclear phagocytes, some endothelial cells, thymic epithelial cells, and B cells. The antigens presented by class II peptides are derived from extracellular proteins. Expression of antigen presentation related genes, including MHC I, MHC II related genes, are compared between tumors with and without ecDNA (Fig. 5a and Supplementary Fig. S6). In tumors with ecDNA significantly decreased expression of MHC class I and class II genes are observed (Fig. 5a). Gene set enrichment analysis indicates MHC class I and class II related genes are significantly down-regulated in tumors with ecDNA in pan-cancer dataset (Fig. 5b). The impaired expression of MHC I and II related antigen presentation genes could be the mechanism underlying decreased immune infiltration in tumors with ecDNA.

## Discussion

Here we provide evidence to show that the presence of ecDNA is associated with decreased immune cell infiltration, decreased cytotoxic T cell percentage/composition, decreased expression of both class I and class II antigen presentation machinery genes. This analysis indicates that ecDNA formation could be one of the mechanisms employed by tumor cells to evade immune surveillance. EcDNA is preferentially detected in tumors, and less frequently in cultured tumor cells<sup>27</sup>. The immune selection pressure in tumors could be the underlying mechanism for this observation.

This study is based on gene expression data derived from bulk tumor samples, currently it is unclear if the gene expression differences happens in tumor cells or in the microenvironment immune cells or stromal cells. Consistently down-regulated antigen presentation related genes are observed in various types of tumors with ecDNA, and the functional consequence of these gene expression down-regulation in antigen presentation process need to be examined using experimental assays.

Based on this study ecDNA could directly induce tumor immune escape through down-regulating the expression of antigen presentation genes. Currently there are no experimental evidences supporting the alternative hypothesis that immunosuppressive microenvironment directly induces ecDNA formation. Potential inducers for ecDNA formation include DNA repair defect, telomere shortening, cell cycle defects, and most of these ecDNA inducers are cell-intrinsic defects<sup>28,29</sup>.

The detailed molecular mechanism responsible for the decreased MHC class I and II antigen presentation genes' expression, and immune evasion in ecDNA-containing tumors is not clear. The ecDNA associated oncogene could be a potential mechanism. The function of nuclear circular DNA on immune response is unknown. Cytoplasmic DNA is known to stimulate immune response through cGAS-STING pathway<sup>30</sup>, and in tumors with ecDNA, this pathway is not over-activated (Supplementary Fig. S7). EcDNA formation is a type of genomic DNA copy number alteration, its detections with copy number signature analysis could reveal potentially actionable biomarkers for cancer precision therapy<sup>31–33</sup>. Tumors with ecDNA are known to have poorer prognosis



**Figure 2.** ecDNA and the infiltration of different types of immune cells. **(a)** Comparisons of the compositions of different types of immune cells between tumors with ecDNA and without ecDNA. The immune cell compositions have been quantified by five different methods, including Cibersort, Xcell, Timer, MCPcounter and Quantiseq. Wilcoxon test *P* values are shown. ns:  $P > 0.05$ , \*:  $P \leq 0.05$ , \*\*:  $P \leq 0.01$ , \*\*\*:  $P \leq 0.001$ , \*\*\*\*:  $P \leq 0.0001$ . **(b)** Comparison of immune cell infiltration levels quantified by five different methods between ecDNA and non-ecDNA samples in different cancer types. Heatmap color indicates ratio of the median infiltration level for specific immune cell and specific cancer type between ecDNA and non-ecDNA samples. TCGA cancer type acronyms: STAD (stomach adenocarcinoma), SKCM (skin cutaneous melanoma), HNSC (head and neck squamous cell carcinoma), LUAD (lung adenocarcinoma), BLCA (bladder urothelial carcinoma), BRCA (breast invasive carcinoma), ESCA (esophageal carcinoma).

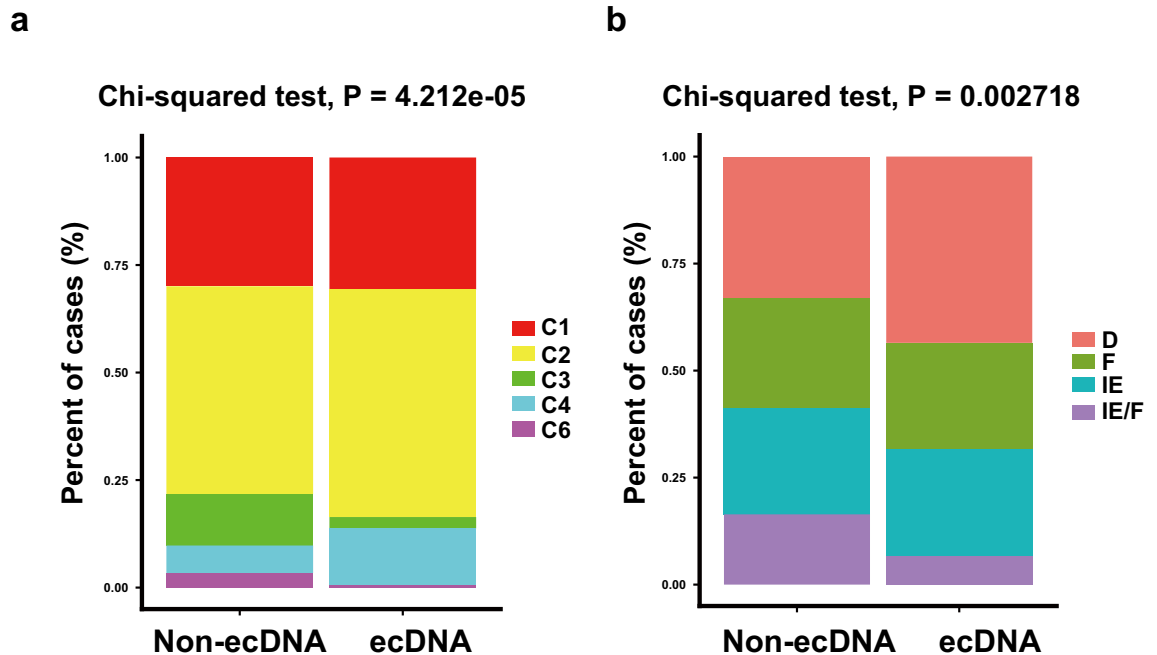


**Figure 3.** ecDNA and tumor immune typing. **(a)** TME classification in tumors with and without ecDNA according to Thorsson et al. method. Chi-squared test *P* value is shown. C1: wound healing; C2: IFN- $\gamma$  dominant; C3: inflammatory; C4: lymphocyte depleted; C5: immunologically quiet; C6: TGF- $\beta$  dominant. **(b)** Immune type classification in tumors with ecDNA and without ecDNA according to Bagaev et al. method. Chi-squared test *p* value is shown. *D* immune-depleted; *F* fibrotic; *IE* immune-enriched, non-fibrotic; *IE/F* immune-enriched, fibrotic.

compared with tumors without ecDNA<sup>17</sup>. Stimulating the antigen presentation pathway could potentially revert the ecDNA-mediated immune escape.

## Materials and methods

**Data source.** EcDNA status information was determined using AmpliconArchitect from whole genome sequencing (WGS) data as described previously<sup>17</sup>. Gene expression data are available for the majority of the cancer genome atlas (TCGA) but not pan-cancer analysis of whole genomes (PCAWG) datasets. For downstream immune infiltration and gene expression analysis, we only keep TCGA samples. Tumor immune cell infiltration information for TCGA samples was downloaded from the TIMER webserver (<http://timer.comp-genomics.org/>), including the results calculated by TIMER, CIBERSORT, quanTIseq, xCell, and MCP-counter algorithms. Somatic mutation data detected by Mutect2 was download from UCSC xena (GDC-PANCAN.mutect2\_snv.tsv). The pan-cancer gene-level RNA-Seq data of TCGA samples was downloaded from UCSC xena, including counts and normalized transcripts per million (TPM) data. Immune subtyping and tumor microenvironment (TME) information of TCGA samples are based on reports of Thorsson et al. and Bagaev et al. study respectively<sup>24,25</sup>. The leukocyte fraction data of TCGA samples are based on the results of Thorsson et al. study<sup>25</sup>. In the downstream analysis, we only keep cancer types where the count of ecDNA samples was more than 20. All methods were performed in accordance with the relevant guidelines and regulations.

**Calculation of cancer immune scores.** In addition to immune cell infiltration quantification using gene expression data, we calculated a variety of additional immune microenvironment quantitative scores. The immunophenoscore (IPS) was used to measure the immune state of the samples. IPS was based on the expres-

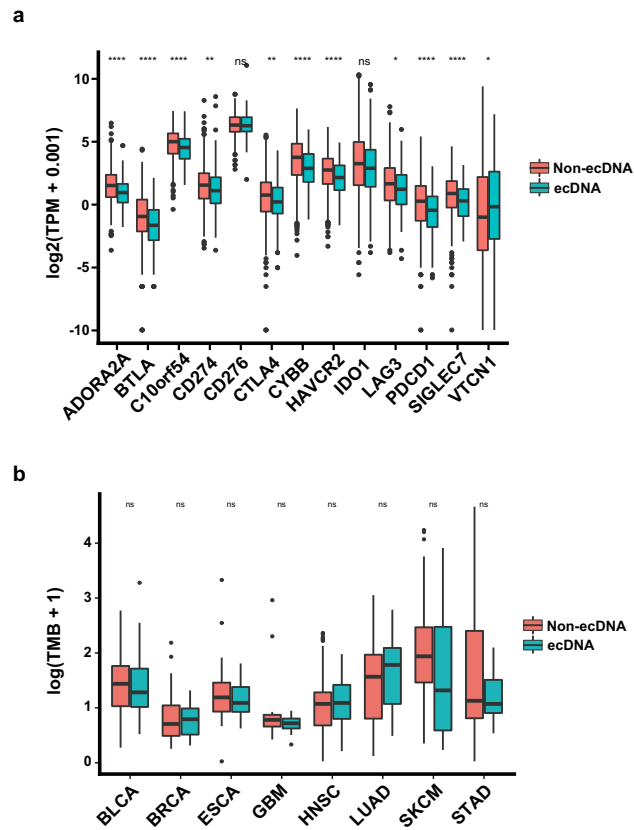


**Figure 4.** ecDNA and expression of inhibitory immune checkpoint genes and TMB. **(a)** Expression of inhibitory immune checkpoint genes in tumors with ecDNA and without ecDNA. Wilcoxon test *P* values are shown. **(b)** Tumor mutation burden (TMB) difference in different types of tumors with and without ecDNA. Wilcoxon test *P* values are shown. ns:  $P > 0.05$ , \*:  $P \leq 0.05$ , \*\*:  $P \leq 0.01$ , \*\*\*:  $P \leq 0.001$ , \*\*\*\*:  $P \leq 0.0001$ . TCGA cancer type acronyms: STAD (stomach adenocarcinoma), SKCM (skin cutaneous melanoma), HNSC (head and neck squamous cell carcinoma), LUAD (lung adenocarcinoma), BLCA (bladder urothelial carcinoma), BRCA (breast invasive carcinoma), ESCA (esophageal carcinoma), GBM (glioblastoma multiforme).

sion of major determinants, identified by a random forest approach, and these factors were classified into four categories: major histocompatibility complex (MHC) molecules, effector cells, suppressor cells and checkpoint markers. We used R scripts and IPS genes provided by the origin paper to calculate IPS scores<sup>34</sup>. ESTIMATE (Estimation of STromal and Immune cells in MAlignant Tumor tissues using Expression data) is a tool using gene signatures to generate three scores: stromal score, immune score and estimate score, we used R package Estimate to calculate the immune score<sup>23</sup>. The cytolytic activity (CYT) score was a quantitative means of assessing cytotoxic T cell infiltration and activity and was calculated as the geometric mean of expression of *GZMA* and *PRF1* genes<sup>35</sup>. The tumor inflammation signature (TIS) uses 18-gene signature to measure a pre-existing but suppressed adaptive immune response within tumors. The TIS has been shown to enrich for patients who respond to the anti-PD1 agent pembrolizumab. TIS was calculated by gene set variation analysis (GSVA) using the 18-gene signature mentioned by Danaher et al.<sup>36</sup>.

**Tumor mutational burden (TMB) and neoantigen burden.** TMB was defined as the number of non-synonymous alterations per megabase (Mb) of genome examined. We used 38 Mb as the estimate of the exome size:  $TMB = (\text{whole exome missense mutations})/38$ . Tumor neoantigen are generated by somatic mutations, and can be recognized as foreign by immune cells, conferring immunogenicity to cancer cells. Neoantigen was predicted based on somatic mutation and human leukocyte antigen (HLA) typing data. HLA typing data for TCGA cancer was obtained from Thorsson et al. study<sup>25</sup>. Mutect2 mutation files were first transformed into VCF format by maf2vcf tools, and we used NeoPredPipe to predict neoantigen<sup>37</sup>. We only evaluated single-nucleotide variants leading to a single amino acid change, and novel peptides of nine amino acids were considered. From the output results, if the IC50 of a novel peptide is less than 50 nM, and the TPM expression level is greater than 1, then this peptide is labeled as neoantigen. A mutation was considered neoantigenic if there was at least a single peptide produced from the mutated base that produce a neoantigen. Neoantigen burden was calculated similarly as TMB: (Total counts of neoantigens in the exome)/38.

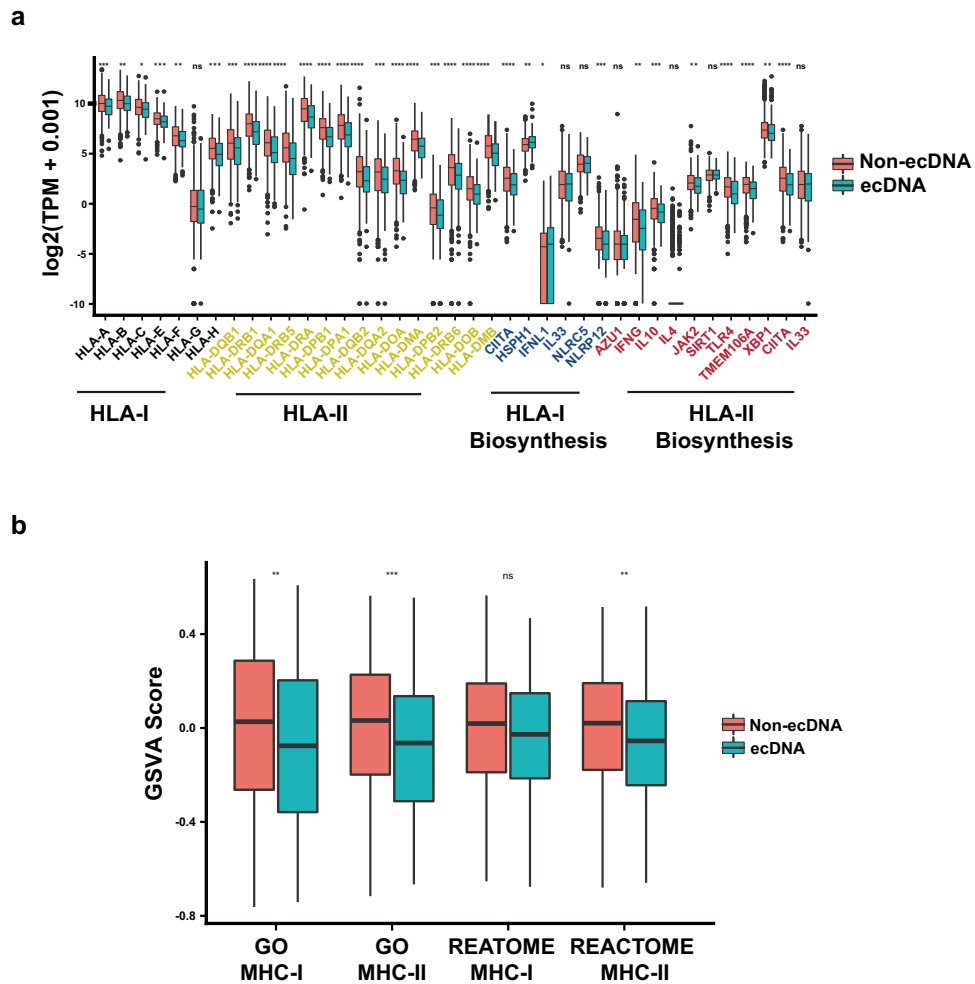


**Figure 5.** ecDNA and antigen presentation genes' expression. **(a)** mRNA expression of MHC class I and class II antigen presentation related genes in tumors with and without ecDNA. Wilcoxon test *P* values are shown. **(b)** GSEA scores of MHC class I or class II antigen presentation genes in tumors with and without ecDNA. Wilcoxon test *P* values are shown. ns:  $P > 0.05$ , \*:  $P \leq 0.05$ , \*\*:  $P \leq 0.01$ , \*\*\*:  $P \leq 0.001$ , \*\*\*\*:  $P \leq 0.0001$ .

**Gene set enrichment analysis (GSEA).** For each cancer type, we used Deseq2 to identify differentially expressed genes between ecDNA and non-ecDNA samples<sup>38</sup>. Then gene set enrichment analysis was performed by using R package "fgsea". We downloaded gene list gmt file for the following pathways from MSigDB database, including "REACTOME\_MHC\_CLASS\_II\_ANTIGEN\_PRESENTATION", "REACTOME\_CLASS\_I\_MHC\_MEDIATED\_ANTIGEN\_PROCESSING\_PRESENTATION", "GOBP\_ANTIGEN\_PROCESSING\_AND\_PRESENTATION\_OF\_PEPTIDE\_ANTIGEN\_VIA\_MHC\_CLASS\_I", and "GOBP\_ANTIGEN\_PROCESSING\_AND\_PRESENTATION\_OF\_PEPTIDE\_OR\_POLYSACCHARIDE\_ANTIGEN\_VIA\_MHC\_CLASS\_II". The GSEA *p* values were corrected by FDR method, and was considered significant if less than 0.05. For each cancer sample, we also calculated corresponding pathway GSEA scores using R package "GSVA"<sup>39</sup>.

**Statistical analysis.** All *P* values showed in boxplot were calculated by Wilcoxon tests using R. We used the following convention for symbols indicating statistical significance: ns:  $P > 0.05$ , \*:  $P \leq 0.05$ , \*\*:  $P \leq 0.01$ , \*\*\*:  $P \leq 0.001$ , \*\*\*\*:  $P \leq 0.0001$ . Immune subtype enrichment analysis was conducted by chi-squared test. All statistical tests and visualization analyses were performed with R.

### Data availability

Only publicly available data were used in this study, and data sources and handling of these data are described in the Materials and Methods and in Supplementary Tables S1–S3. All codes required to reproduce the results reported in this manuscript are freely available at: [https://github.com/XSLiuLab/ecDNA\\_immune](https://github.com/XSLiuLab/ecDNA_immune). Analyses can be read online at: [https://xsluolab.github.io/ecDNA\\_immune/](https://xsluolab.github.io/ecDNA_immune/). Further information is available from the corresponding author upon request.

Received: 30 September 2021; Accepted: 21 February 2022

Published online: 04 March 2022

## References

1. Finn, O. J. Immuno-oncology: Understanding the function and dysfunction of the immune system in cancer. *Ann. Oncol.* **23**, 6–9 (2012).
2. Candéias, S. M. & Gaipal, U. S. The immune system in cancer prevention, development and therapy. *Anti-Cancer Agent Med.* **16**, 101–107 (2016).
3. O'Donnell, J. S., Teng, M. W. L. & Smyth, M. J. Cancer immunoediting and resistance to T cell-based immunotherapy. *Nat. Rev. Clin. Oncol.* **16**, 151–167 (2019).
4. Kim, R., Emi, M. & Tanabe, K. Cancer immunoediting from immune surveillance to immune escape. *Immunology* **121**, 1–14 (2007).
5. Schreiber, R. D., Old, L. J. & Smyth, M. J. Cancer immunoediting: Integrating immunity's roles in cancer suppression and promotion. *Science* **331**, 1565–1570 (2011).
6. Vinay, D. S. *et al.* Immune evasion in cancer: Mechanistic basis and therapeutic strategies. *Semin. Cancer Biol.* **35**, S185–S198 (2015).
7. Restifo, N. P. *et al.* Identification of human cancers deficient in antigen processing. *J. Exp. Med.* **177**, 265–272 (1993).
8. Sade-Feldman, M. *et al.* Resistance to checkpoint blockade therapy through inactivation of antigen presentation. *Nat. Commun.* <https://doi.org/10.1038/s41467-017-01062-w> (2017).
9. Yi, M. *et al.* Synergistic effect of immune checkpoint blockade and anti-angiogenesis in cancer treatment. *Mol. Cancer* **18**, 1–12 (2019).
10. Travis, M. A. & Sheppard, D. TGF-beta activation and function in immunity. *Annu. Rev. Immunol.* **32**, 51–82 (2014).
11. Mariathasan, S. *et al.* TGF beta attenuates tumour response to PD-L1 blockade by contributing to exclusion of T cells. *Nature* **554**, 544–548 (2018).
12. Cox, D., Yuncken, C. & Spriggs, A. I. Minute chromatin bodies in malignant tumours of childhood. *Lancet* **286**, 55–58. [https://doi.org/10.1016/s0140-6736\(65\)90131-5](https://doi.org/10.1016/s0140-6736(65)90131-5) (1965).
13. Liao, Z. Y. *et al.* Classification of extrachromosomal circular DNA with a focus on the role of extrachromosomal DNA (ecDNA) in tumor heterogeneity and progression. *BBA Rev. Cancer* **1874**, 188392 (2020).
14. Turner, K. M. *et al.* Extrachromosomal oncogene amplification drives tumour evolution and genetic heterogeneity. *Nature* **543**, 122–125. <https://doi.org/10.1038/nature21356> (2017).
15. de Carvalho, A. C. *et al.* Discordant inheritance of chromosomal and extrachromosomal DNA elements contributes to dynamic disease evolution in glioblastoma. *Nat. Genet.* **50**, 708–717 (2018).
16. Wu, S. H. *et al.* Circular ecDNA promotes accessible chromatin and high oncogene expression. *Nature* **575**, 699–703 (2019).
17. Kim, H. *et al.* Extrachromosomal DNA is associated with oncogene amplification and poor outcome across multiple cancers. *Nat. Genet.* **52**, 891–897 (2020).
18. Li, T. W. *et al.* TIMER2.0 for analysis of tumor-infiltrating immune cells. *Nucleic Acids Res.* **48**, W509–W514 (2020).
19. Newman, A. M. *et al.* Robust enumeration of cell subsets from tissue expression profiles. *Nat. Methods* **12**, 453–457 (2015).
20. Aran, D., Hu, Z. C. & Butte, A. J. xCell: Digitally portraying the tissue cellular heterogeneity landscape. *Genome Biol.* **18**, 1–14 (2017).
21. Becht, E. *et al.* Estimating the population abundance of tissue-infiltrating immune and stromal cell populations using gene expression. *Genome Biol.* **17**, 1–20 (2016).
22. Finotello, F. *et al.* Molecular and pharmacological modulators of the tumor immune contexture revealed by deconvolution of RNA-seq data. *Genome Med.* **11**, 1–20 (2019).
23. Yoshihara, K. *et al.* Inferring tumour purity and stromal and immune cell admixture from expression data. *Nat. Commun.* **4**, 1–11 (2013).
24. Bagaev, A. *et al.* Conserved pan-cancer microenvironment subtypes predict response to immunotherapy. *Cancer Cell* **39**, 845–865 (2021).
25. Thorsson, V. *et al.* The immune landscape of cancer. *Immunity* **48**, 812–830 (2018).
26. Wang, S. X., He, Z. K., Wang, X., Li, H. M. & Liu, X. S. Antigen presentation and tumor immunogenicity in cancer immunotherapy response prediction. *Elife* **8**, e49020 (2019).
27. Tandon, I., Pal, R., Pal, J. K. & Sharma, N. K. Extrachromosomal circular DNAs: An extra piece of evidence to depict tumor heterogeneity. *Future Sci. OA* <https://doi.org/10.2144/fsoa-2019-0024> (2019).
28. Verhaak, R. G. W., Bafna, V. & Mischel, P. S. Extrachromosomal oncogene amplification in tumour pathogenesis and evolution. *Nat. Rev. Cancer* **19**, 283–288 (2019).
29. Wu, S., Bafna, V., Chang, H. Y. & Mischel, P. S. Extrachromosomal DNA: An emerging hallmark in human cancer. *Annu. Rev. Pathol. Mech. Dis.* **17**, 367–386. <https://doi.org/10.1146/annurev-pathmechdis-051821-114223> (2022).
30. Chen, Q., Sun, L. J. & Chen, Z. J. Regulation and function of the cGAS-STING pathway of cytosolic DNA sensing. *Nat. Immunol.* **17**, 1142–1149 (2016).
31. Wang, S. X. *et al.* Copy number signature analysis tool and its application in prostate cancer reveals distinct mutational processes and clinical outcomes. *PLoS Genet.* <https://doi.org/10.1371/journal.pgen.1009557> (2021).
32. Wang, S. X., Tao, Z. Y., Wu, T. & Liu, X. S. Sigflow: An automated and comprehensive pipeline for cancer genome mutational signature analysis. *Bioinformatics* **37**, 1590–1592 (2021).
33. Wang, S. *et al.* UCSCXenaShiny: An R/CRAN package for interactive analysis of UCSC Xena data. *Bioinformatics* <https://doi.org/10.1093/bioinformatics/btab561> (2021).
34. Charoentong, P. *et al.* Pan-cancer immunogenomic analyses reveal genotype-immunophenotype relationships and predictors of response to checkpoint blockade. *Cell Rep.* **18**, 248–262 (2017).
35. Rooney, M. S., Shukla, S. A., Wu, C. J., Getz, G. & Hacohen, N. Molecular and genetic properties of tumors associated with local immune cytolytic activity. *Cell* **160**, 48–61 (2015).
36. Danaher, P. *et al.* Pan-cancer adaptive immune resistance as defined by the tumor inflammation signature (TIS): Results from the cancer genome atlas (TCGA). *J. Immunother. Cancer* **6**, 1–17 (2018).
37. Schenk, R. O., Lakatos, E., Gatenbee, C., Graham, T. A. & Anderson, A. R. A. NeoPredPipe: High-throughput neoantigen prediction and recognition potential pipeline. *Bmc Bioinform.* **20**, 1–6 (2019).
38. Love, M. I., Huber, W. & Anders, S. Moderated estimation of fold change and dispersion for RNA-seq data with DESeq2. *Genome Biol.* **15**, 1–21 (2014).
39. Hanzelmann, S., Castelo, R. & Guinney, J. GSEA: Gene set variation analysis for microarray and RNA-Seq data. *Bmc Bioinform.* **14**, 1–15 (2013).



## Acknowledgements

We thank ShanghaiTech University High Performance Computing Public Service Platform for computing services. We thank Raymond Shuter for editing the text. We thank multi-omics facility, molecular and cell biology core facility of ShanghaiTech University for technical help. This work was supported by Shanghai Science and Technology Commission (21ZR1442400), the National Natural Science Foundation of China (31771373), and startup funding from ShanghaiTech University.

## Author contributions

T.W., C.W., collected the data and performed the computational analysis. X.Z., G.W., W.N., Z.T., F.C. participated in critical project discussion. X.S.L. designed, supervised the study and wrote the manuscript.

## Competing interests

The authors declare no competing interests.

## Additional information

**Supplementary Information** The online version contains supplementary material available at <https://doi.org/10.1038/s41598-022-07530-8>.

**Correspondence** and requests for materials should be addressed to X.-S.L.

**Reprints and permissions information** is available at [www.nature.com/reprints](http://www.nature.com/reprints).

**Publisher's note** Springer Nature remains neutral with regard to jurisdictional claims in published maps and institutional affiliations.



**Open Access** This article is licensed under a Creative Commons Attribution 4.0 International License, which permits use, sharing, adaptation, distribution and reproduction in any medium or format, as long as you give appropriate credit to the original author(s) and the source, provide a link to the Creative Commons licence, and indicate if changes were made. The images or other third party material in this article are included in the article's Creative Commons licence, unless indicated otherwise in a credit line to the material. If material is not included in the article's Creative Commons licence and your intended use is not permitted by statutory regulation or exceeds the permitted use, you will need to obtain permission directly from the copyright holder. To view a copy of this licence, visit <http://creativecommons.org/licenses/by/4.0/>.

© The Author(s) 2022